JMEMS Letters

Coupling of Lamb Waves and Spin Waves in Multiferroic Heterostructures

Sidhant Tiwari, *Member, IEEE*, Joseph D. Schneider, Sebastian Wintz, Sri S. P. K. Arekapudi, *Member, IEEE*, Kilian Lenz, Andres Chavez, Jürgen Lindner, Olav Hellwig, Greg P. Carman, and Robert N. Candler, *Senior Member, IEEE*

***Abstract*—In this work, we investigate magneto-acoustic attenuation in thin film multiferroic Lamb wave delay lines. By leveraging magneto-acoustic interactions, multiferroics have potential to realize passive chip-scale alternatives to bulky ferrite devices. For the first time, magnetic field dependence of magneto-acoustic interactions in multiferroic Lamb wave devices is characterized. Multiferroic heterostructures of aluminum nitride and cobalt iron boron are fabricated into Lamb wave delay lines operating at 7.492 GHz to study the effect of strain nonuniformity on the multiferroic coupling. The attenuation of the Lamb waves is characterized as a function of the magnitude and angle of an applied in-plane bias magnetic field. It is found that the bias magnitude for peak attenuation is a strong function of angle, indicating that it is due to coupling between the Lamb waves and spin wave modes. This is in contrast with current models of attenuation in multiferroic SAW delay lines, where the uniform surface strains couple to ferromagnetic resonance, which has no angular dependence on the in-plane bias field magnitude. These results are the first steps towards passive chip-scale alternatives to ferrite devices utilizing Lamb wave devices, which have better coupling and scalability than their SAW counterparts. [2020-0114]**

***Index Terms*—Acoustic delay lines, Lamb waves, magneto-acoustics, MEMS, multiferroics, spin waves.**

I. Introduction

Circulators, isolators, and other devices that leverage the unique interactions of electromagnetic (EM) waves with magnetic materials are pervasive throughout radio frequency (RF) systems [1]. Despite decades of miniaturization of RF electronics, these magnetic components have not seen nearly as dramatic of a size reduction and are currently the bulkiest components in RF front ends [2]. Since these devices rely on EM waves for operation, their dimensions must be on par with the EM wavelength to have any appreciable effect.

Magneto-acoustic technology offers a route for the miniaturization of magnetic devices used in RF systems by instead leveraging the interactions of acoustic waves with magnetic materials. Due to the approximately five orders-of-magnitude difference between the speed of light and the speed of acoustic waves, utilizing magneto-acoustics will lead to dramatic size reduction in device characteristic length.

To enable these magneto-acoustic devices, a new class of devices called multiferroics can be leveraged [3], [4]. These systems couple magnetostrictive and piezoelectric materials through strain to enable electric field control of micro-magnetic devices. Prior work in micro-scale magneto-acoustics has primarily focused on multiferroic surface acoustic wave (SAW) devices [5], [6]. In these devices the strains are approximately uniform through the thickness of the magnetic film, meaning only the uniform magnetization oscillation mode, known as ferromagnetic resonance (FMR), is driven. However, pushing magneto-acoustic devices to higher frequencies will require shorter wavelengths, resulting in nonuniform strains and coupling to nonuniform magnetic modes, called spin waves. Preliminary investigation of the effect of strain nonuniformity in multiferroic SAW devices has been done [7]. However, SAW devices have low phase velocities, limiting their scalability to higher frequencies due to the small lithographic features needed [8]. Lamb waves are much better suited for higher frequencies due to the faster phase velocities, access to higher-order modes, and higher electromechanical coupling [8]–[10]. While Lamb waves can be dispersive, especially higher-order modes, it has been shown that this dispersion can be compensated by using chirped signals [11], which can be excited in thin film plates through the electrode design [12]. As first steps towards high frequency magneto-acoustic devices, this work presents the measurement of spin wave damping of acoustic waves in a multiferroic Lamb wave delay line. The significance of this result is that it experimentally shows, for the first time, the dependence of Lamb wave/spin wave coupling in thin film multiferroic heterostructures on external magnetic fields.

II. Background

The magnetic film thickness in a multiferroic SAW device is small compared to the acoustic wavelength and the substrate, so the strain in the magnetic film is approximately uniform throughout its thickness and drives the FMR mode in the magnetic layer. In composite Lamb wave delay lines (Fig. 1), the magnetic material is a significant portion of the device cross section. The strains now can no longer be assumed to be uniform and spin waves are excited instead of FMR.

Spin wave modes have unique properties that are not present in ferromagnetic resonance, one being that the magnetic field required for the existence of the spin wave mode, for a fixed wave number and frequency, is strongly dependent on the angle between the spin wave propagation direction and the bias magnetic field applied, even

Manuscript received May 1, 2020; revised July 14, 2020; accepted July 18, 2020. Date of publication August 28, 2020; date of current version October 7, 2020. This work was supported by the National Science Foundation through the Cooperative Agreement for Solicitation NSF 11-537 (TANMS) managed by Dr. Sandra Cruz-Pol under Award EEC-1160504. Subject Editor M. Rais-Zadeh. *(Corresponding authors: Sidhant Tiwari; Robert N. Candler.)*

Sidhant Tiwari is with the Department of Electrical and Computer Engineering, University of California at Los Angeles, Los Angeles, CA 90095 USA (e-mail: stiwari@ucla.edu).

Joseph D. Schneider and Greg P. Carman are with the Department of Mechanical and Aerospace Engineering, University of California at Los Angeles, Los Angeles, CA 90095 USA.

Sebastian Wintz is with the Paul Scherrer Institut, 5232 Villigen, Switzerland.

Sri S. P. K. Arekapudi is with the Institute of Physics, Chemnitz University of Technology, 09111 Chemnitz, Germany.

Kilian Lenz and Jürgen Lindner are with the Institute of Ion Beam Physics and Materials Research, Helmholtz-Zentrum Dresden-Rossendorf, 01328 Dresden, Germany.

Andres Chavez was with the Department of Mechanical and Aerospace Engineering, University of California at Los Angeles, Los Angeles, CA 90095 USA. He is now with Northrop Grumman Corporation, Falls Church, VA 22042 USA.

Olav Hellwig is with the Institute of Physics, Chemnitz University of Technology, 09111 Chemnitz, Germany, and also with Institute of Ion Beam Physics and Materials Research, Helmholtz-Zentrum Dresden-Rossendorf, 01328 Dresden, Germany.

Robert N. Candler is with the Electrical and Computer Engineering Department, University of California at Los Angeles, Los Angeles, CA 90095 USA, and also with the California NanoSystems Institute (CNSI), Los Angeles, CA 90095 USA (e-mail: rcandler@ee.ucla.edu).

Color versions of one or more of the figures in this article are available online at http://ieeexplore.ieee.org.

Digital Object Identifier 10.1109/JMEMS.2020.3017138

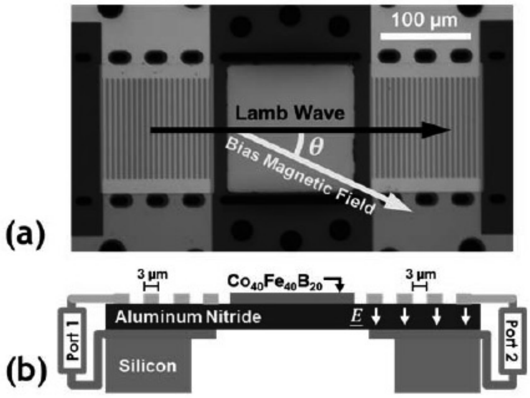

Fig. 1. (a) Microscope image of a fabricated multiferroic Lamb wave delay line and (b) diagram of the device cross section. The angle between the Lamb wave propagation direction and the applied bias magnetic field is θ.

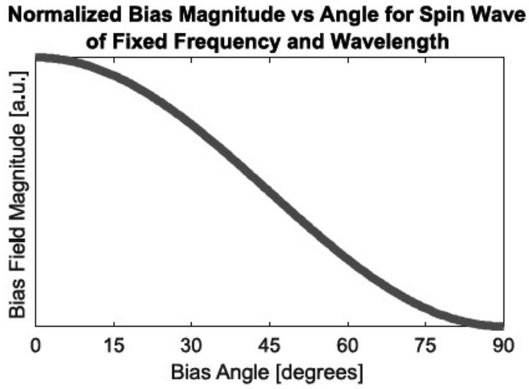

Fig. 2. Dependence of the H_{bias}/M_s needed for the existence of a spin wave mode as a function of the angle between the bias magnetic field and the spin wave propagation direction, with frequency and wavelength fixed.

if the magnetic film is isotropic. Angular dependence in FMR is only possible with material anisotropy, caused by either the shape or crystal structure. Neglecting the influence of the magnetic film's thickness, this is approximately shown by the equation below [13].

$$H_{bias} = \frac{\omega - \eta k^2}{\gamma \mu_0} - \frac{1}{2} M_s \sin^2 \theta \tag{1}$$

Here ω is the angular frequency, γ is the gyromagnetic constant, η is the exchange constant, k is the wave number, M_s is the saturation magnetization, and H_{bias} and θ are the bias magnitude and bias angle relative to the spin wave propagation direction, respectively. The trend for H_{bias}/M_s versus angle, for fixed frequency and wave number, is plotted in Fig. 2. As the bias angle increases, the bias magnitude needed for the spin wave mode to exist decreases as $-sin^2\theta$.

III. Experiment

To investigate coupling of spin waves with acoustic waves, Lamb wave delay lines were fabricated, with 400 nm of aluminum nitride (AlN) as the piezoelectric layer and 70 nm of amorphous cobalt iron boron ($Co_{40}Fe_{40}B_{20}$) (144 μm × 144 μm in-plane) as the magnetostrictive layer (Fig. 1). As the in-plane dimensions of the $Co_{40}Fe_{40}B_{20}$ are much larger than the thickness, edge effects are weak and it is regarded as isotropic. As the $Co_{40}Fe_{40}B_{20}$ is a major portion of the device cross section, strains are not uniform through its thickness, resulting in nonuniform driving fields within the magnetic layer. Parallel plate electrodes were used instead of traditional IDTs to excite higher frequencies while still using contact lithography, at the cost of the electromechanical coupling.

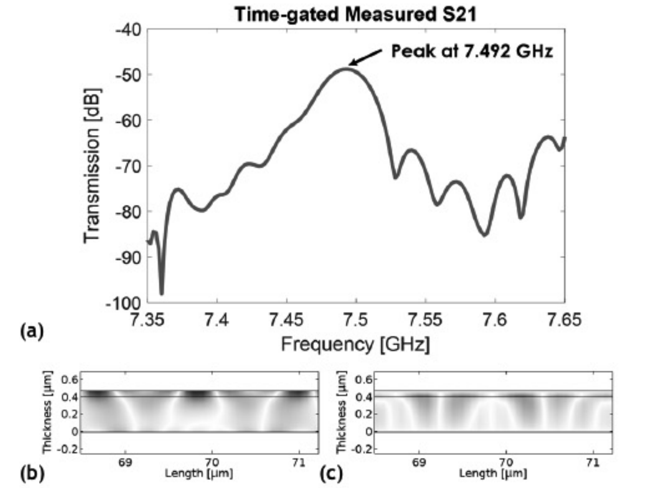

Fig. 3. (a) Measured S21 of the Lamb wave delay line at mode of interest. Simulated in-plane (b) extensional and (c) shear strain profiles of the mode.

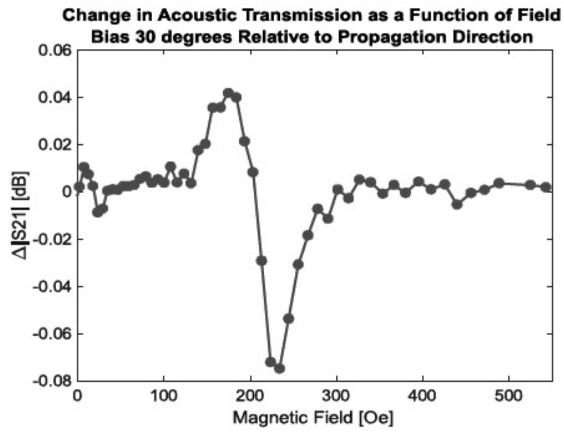

Fig. 4. Change in S21 of the chosen acoustic mode, 7.492 GHz, as a function of DC magnetic bias field at an angle of 30°. Attenuation of the acoustic wave by the magnetic thin film maximizes near 230 Oe, indicating the presence of a spin wave mode that matches the acoustic wave wavelength and frequency.

To further enhance the nonuniformity of the strain fields, the device is run at a high harmonic to shorten the wavelength. For this experiment, a Lamb mode at 7.492 GHz is chosen (Fig. 3a). The wavelength is approximately 1.5 μm. Due to the presence of the $Co_{40}Fe_{40}B_{20}$ layer, the Lamb wave is perturbed from a symmetric mode to a quasi-symmetric mode (Fig. 3b,c).

The Lamb wave device is placed in an electromagnet which applies an in-plane bias magnetic field at several different magnitudes and angles. The angle is controlled using a Thorlabs CR1 manual continuous rotation stage, measuring the angular position with the radial scale. The field modifies the frequencies and wave numbers of the spin wave modes in the $Co_{40}Fe_{40}B_{20}$ layer. At each combination of magnetic field magnitude and angle, the device S-parameters are measured using a PNA-L network analyzer, with the IF bandwidth set to 500 Hz and averaging set to 10 to minimize random S21 variation. The impact of EM feedthrough and acoustic reflections is minimized by time-gating the signal between 23 ns and 60 ns.

IV. Results

Shown in Fig. 4 is a representative plot of the measured magnetic field dependent change of the S21 at 7.492 GHz. As the magnetic field is increased, eventually the spin wave matches the acoustic wave

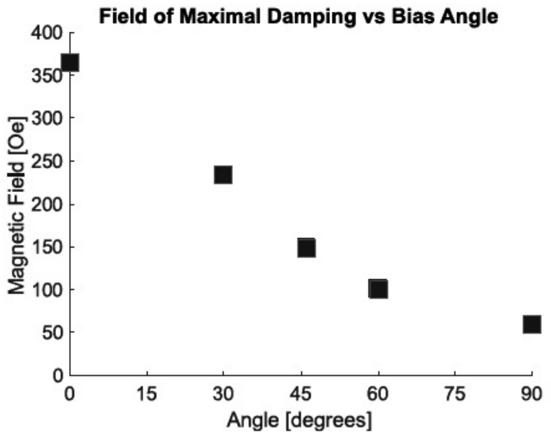

Fig. 5. Measured bias magnitude of maximum acoustic wave damping versus the angle of the magnetic field. As the angle increases, the bias needed decreases, matching the trend shown in Fig. 2. This is a unique aspect of coupling to spin wave modes, only achievable by using nonuniform strains.

in wavelength and frequency. This leads to increased damping of the acoustic wave as energy is dissipated by the spin wave and manifests itself as a dip in the S21 (230 Oe in Fig. 4). The peak is likely caused by an increase in acoustic wave velocity from the magneto-acoustic back-action [14]. The bias magnetic field at which this dip occurs for each angle of the experiment is plotted in Fig. 5. As the angle of the magnetic field increases, the bias field of the maximal damping point decreases, which is the same trend as predicted for the spin wave dispersion (Fig. 2). This is in stark difference with previous work in SAW driven FMR, where the bias magnitude for maximal damping show no dependence on the angle for isotropic materials [5], [6]. These findings are key first steps towards the realization of high frequency magneto-acoustic devices where the short acoustic wavelengths will necessitate coupling to spin wave modes instead of FMR.

Acknowledgment

The authors would like to thank the Center for High Frequency Electronics, the UCLA Nanoelectronics Research Facility, and the Integrated Systems Nanofabrication Cleanroom for their assistance with the experimental portions of this work.

References

[1] D. M. Pozar, *Microwave Engineering*, 4th ed. Hoboken, NJ, USA: Wiley, 2012.

[2] W. Palmer, D. Kirkwood, S. Gross, M. Steer, H. S. Newman, and S. Johnson, “A bright future for integrated magnetics: Magnetic components used in microwave and mm-Wave systems, useful materials, and unique functionalities,” *IEEE Microw. Mag.*, vol. 20, no. 6, pp. 36–50, Jun. 2019, doi: 10.1109/MMM.2019.2904381.

[3] G. P. Carman and N. Sun, “Strain-mediated magnetoelectrics: Turning science fiction into reality,” *MRS Bull.*, vol. 43, no. 11, pp. 822–828, Nov. 2018, doi: 10.1557/mrs.2018.236.

[4] C.-W. Nan, M. I. Bichurin, S. Dong, D. Viehland, and G. Srinivasan, “Multiferroic magnetoelectric composites: Historical perspective, status, and future directions,” *J. Appl. Phys.*, vol. 103, no. 3, Feb. 2008, Art. no. 031101, doi: 10.1063/1.2836410.

[5] D. Labanowski, A. Jung, and S. Salahuddin, “Power absorption in acoustically driven ferromagnetic resonance,” *Appl. Phys. Lett.*, vol. 108, no. 2, Jan. 2016, Art. no. 022905, doi: 10.1063/1.4939914.

[6] L. Dreher *et al.*, “Surface acoustic wave driven ferromagnetic resonance in nickel thin films: Theory and experiment,” *Phys. Rev. B, Condens. Matter*, vol. 86, no. 13, Oct. 2012, Art. no. 134415, doi: 10.1103/PhysRevB.86.134415.

[7] S. Tateno and Y. Nozaki, “Highly nonreciprocal spin waves excited by magnetoelastic coupling in a Ni / Si bilayer,” *Phys. Rev. A, Gen. Phys. Appl.*, vol. 13, no. 3, Mar. 2020, Art. no. 034074, doi: 10.1103/physrevapplied.13.034074.

[8] S. Gong and G. Piazza, “Design and analysis of lithium–niobate-based high electromechanical coupling RF-MEMS resonators for wideband filtering,” *IEEE Trans. Microw. Theory Techn.*, vol. 61, no. 1, pp. 403–414, Jan. 2013, doi: 10.1109/TMTT.2012.2228671.

[9] G. Chen and M. Rinaldi, “Aluminum nitride combined overtone resonators for the 5G high frequency bands,” *J. Microelectromech. Syst.*, vol. 29, no. 2, pp. 148–159, Apr. 2020, doi: 10.1109/JMEMS.2020.2975557.

[10] Y. Yang, R. Lu, T. Manzaneque, and S. Gong, “Toward Ka band acoustics: Lithium niobate asymmetrical mode piezoelectric MEMS resonators,” in *Proc. IEEE Int. Freq. Control Symp. (IFCS)*, May 2018, pp. 65–69, doi: 10.1109/FCS.2018.8597475.

[11] L. Zeng and J. Lin, “Chirp-based dispersion pre-compensation for high resolution Lamb wave inspection,” *NDT E Int.*, vol. 61, pp. 35–44, Jan. 2014, doi: 10.1016/j.ndteint.2013.09.008.

[12] T. Manzaneque, R. Lu, Y. Yang, and S. Gong, “Lithium niobate MEMS chirp compressors for near zero power wake-up radios,” *J. Microelectromech. Syst.*, vol. 26, no. 6, pp. 1204–1215, Dec. 2017, doi: 10.1109/JMEMS.2017.2750176.

[13] A. G. Gurevich and G. A. Melkov, *Magnetization Oscillations and Waves*. Boca Raton, FL, USA: CRC Press, 1996.

[14] J. P. Parekh and H. L. Bertoni, “Magnetoelastic Rayleigh waves propagating along a tangential bias field on a YIG substrate,” *J. Appl. Phys.*, vol. 45, no. 1, pp. 434–445, Jan. 1974, doi: 10.1063/1.1662999.